 FDMP, vol.9, no.1, pp.11-21, 2013

An Alternative Approach to Minimize the Convection in Growing a Large Diameter Single Bulk Crystal of $Si_{0.25}Ge_{0.75}$ Alloy in a Vertical Bridgman Furnace

M. M. Shemirani[1] **and M. Z. Saghir**[2]

Abstract: Producing homogeneous single bulk crystals requires a good understanding of the thermo-solutal behavior in the solvent region. This study explores simulation of the growth of large diameter single bulk crystals of silicon and germanium alloy from its melt utilizing Bridgman method. Both thermal and solutal diffusion of silicon and germanium in the molten SiGe alloy are of interest. It was observed that the diffusion dominates the transport phenomenon in the solvent region especially in the first 25 mm of the model due to having a $Pe_T << 1$. It was also found that the control of both radial and axial applied temperature can be considered as an alternative approach to obtain a homogeneous and uniform distribution of silicon in the solvent region, more specifically near the solid liquid interface. This of course was accompanied by applying a reduced pulling rate. The aforementioned parameters are integral part of obtaining a flat or near flat shape interface which is most sought after in industry.

Keywords: Crystal Growth, Thermal Gradient, Silicon-Germanium, Bridgman.

1 Introduction

The reliability of the today's electronic devices and products is highly depending on the performance of the semiconductors being used in them. This reliance is based on the consistency of internal arrangement of atoms of three dimensional crystal structure and the characteristics such as uniformity and purity of bulk single crystals. Silicon-germanium alloys are rapidly becoming an important semiconductor material, for use in high speed integrated circuits. Circuits utilizing the properties of SiGe junctions can be much faster than those using silicon alone. Silicon-germanium is beginning to replace gallium arsenide (GaAs) in wireless

[1] ALHOSN University, Abu Dhabi, UAE
[2] Ryerson University, Toronto, ON, Canada

communications devices. The SiGe chips, with high-speed properties, can also be made.

One of the purposes of this study is to find a proper condition in terrestrial condition which SiGe chips can be obtained from a defect free single crystal of SiGe by utilizing the Bridgam technique. In this technique the polycrystalline is heated above its melting point and slowly being cooled from one end of its container, in vertical Bridgman, it is from the bottom side of it where a seed crystal is placed.

Although the pure silicon and germanium are chemically similar, crystallize in the same lattice structure, and are completely miscible in the solid and liquid phase, the growth of mixed crystals is very complicated because of the differences in some physical properties especially when the combination is in the wider range in the phase diagram, O'Mara, William (1990). The gravity has a great influence on the growth process since it is the major cause of the buoyancy force which in turn affects on the mass and heat transport mechanisms in each system (melt) of crystal growth. It has been observed that the intensity of the melt convection has a significant influence on both radial and axial segregation of species and interface shape during crystal growth. Studies of natural convection in the melt demonstrated that the magnitude of radial segregation is lower than the axial one and is due to either; a) diffusion-controlled growth such as convection free or b) intense mixing in the melt as per Nikitin, Polezhayev, and Fedyushkin (1981) as well as Chang, and Brown (1983). In the vertical Bridgman configuration for crystal growth, the interface shape is a factor that greatly influences the yield of single crystals. The shape of the interface is mainly determined by the temperature field near the interface and the level of natural convection in the melt as stated by Meyer, Ostrogorsky (1997) and Jasinsky, Witt (1984).

The shape of the interface can range from concave to convex. Slightly convex interface shape is most desirable because it eliminates most problems with spontaneous nucleation at the crucible wall and improves grain selection which results in higher yield of single crystals. However, the efforts of obtaining convex interface shapes in growth experiments have been of limited success as shown by Fu, Wilcox (1980).

In this paper we are attempting to investigate the effects of both axial and radial temperature on the growth of $Si_{0.25}Ge_{0.75}$ by utilizing the Bridgman technique. One great feature of the Bridgman technique is that the interfacial temperature gradient and interface position can independently be adjusted according to Chong, Wilcox (1974).

There are other methods to suppress the convection in the solvent region such as microgravity and or applied magnetic field which have been addressed before by other researchers such as Feonychev (2004) and Walker (1998). Application of lin-

ear temperature profile on the solvent region in semiconductor crystal growth with proposed temperature gradient is an alternative approach to control the convection in the liquid.

2 Model Description

The model consists of a fixed cylindrical coordinate system of (r, ϕ, z) with its origin located at the center of the solid section (seed). The model is 11.5cm long with a uniform diameter of 2.5 cm and consists of two segments as; seed (Silicon) 2.5 cm, the solvent region 9.0 cm which is a mixture of silicon (Si) and germanium (Ge) initially set as $Ge_{0.75}$ $Si_{0.25}$, which is the upper segment. The vertical Bridgman method is the technique being chosen for this study. Both sections, introduced earlier in model description, are held in a quartz ampoule. A linear temperature gradient with minimal temperature difference between top and the bottom of the model is applied on the outer face of the crucible. Since the melt temperature of the solvent region is much less than that of the quartz, therefore there would be no oxygen penetration from quartz into the melt and consequently no contamination or impurity occurs which is a great advantage of low temperature gradient in this technique. Fig.1 depicts the model under this study.

2.1 Boundary condition

In this model, the boundary conditions are as follow:

a) At the ampoule side wall (solid), the velocity components are considered as:

u = 0, v = 0 and w = 0 (Non-slip condition) $\frac{\partial c}{\partial r} = 0$ and T= Linear profile applied on side walls, where: $\frac{\partial c}{\partial r}$ is the solutal gradient.

b) At the dissolution interface which is on the top horizontal plane;

c = c_1 = 0.34, and T = defined as per case

c) At the solid interface which is on the bottom horizontal plane;

c = c_2 = 0.25, and T = 1057.5 °C

Where c_1 and c_2 are representing the silicon concentration at the dissolution and soli-liquid interface respectively.

At the external surface of the quartz ampoule (not shown in the Fig. 1) a linear temperature distribution is applied uniformly in the axial direction. It should be noted that we have assumed that the boundary condition is applied on the sample external surface and the quartz tube has not be taken into the consideration in our modeling.

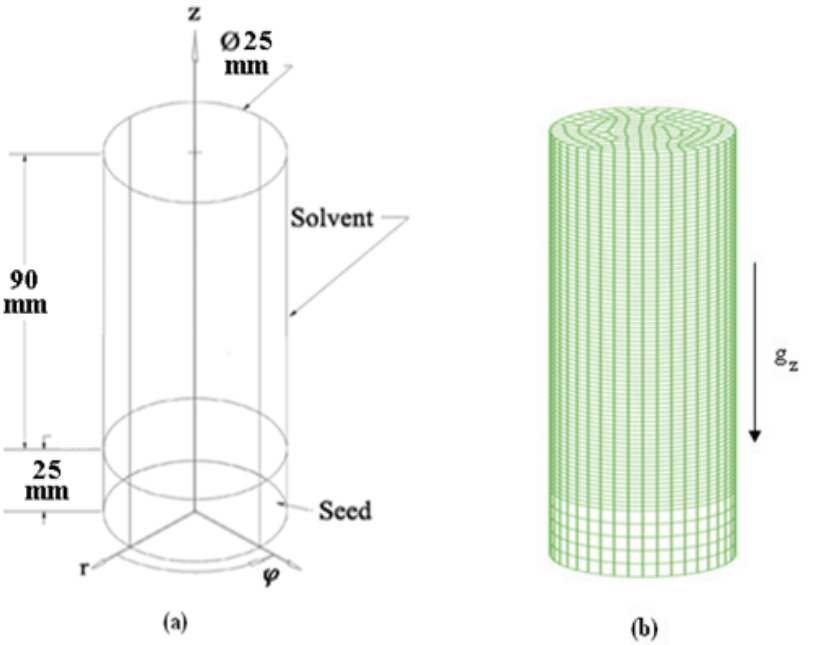

Figure 1: Bridgman model region under the investigation **a)** Coordinates and Model Geometry **b)** Meshed Model

3 Governing Equations

3.1 Momentum Equations

The full set of Navier-Stokes equations for laminar and transient condition for an incompressible Newtonian flows, by taking the Boussinesq approximation into the consideration are solved for radial (r), circumferential (ϕ) and vertical (z) axis respectively and are presented in the non-dimensional forms as:

r-Component

$$Re\left((U.\nabla)U-\frac{V^2}{R}\right)=-\frac{\partial P}{\partial R}\left(\nabla^2 U-\frac{U}{R^2}-\frac{2}{R^2}\frac{\partial V}{\partial \Phi}\right)+\frac{(Gr_T)_r}{Re}\theta-\frac{(Gr_c)_r}{Re}C \quad (1)$$

ϕ-Component

$$Re\left((U.\nabla)V-\frac{UV}{R}\right)=-\frac{1}{R}\frac{\partial P}{\partial \Phi}\left(\nabla^2 \mathrm{V}-\frac{\mathrm{V}}{R^2}+\frac{2}{R^2}\frac{\partial \mathrm{V}}{\partial \Phi}\right)+\frac{(Gr_T)_r}{Re}\theta-\frac{(Gr_c)_r}{Re}C \quad (2)$$

z-Component

$$Re\left((U.\nabla)W\right) = -\frac{\partial P}{\partial R} + \left(\nabla^2 \mathrm{W}\right) + \frac{(Gr_T)_r}{Re}\theta - \frac{(Gr_c)_r}{Re}\,C \tag{3}$$

Where; U, V, W, are dimensionless components of velocity in radial (R), circumferential (Φ), and axial (Z) direction respectively.

3.2 Energy Equation

The energy equation for the solvent region is described as:

$$(U.\nabla)\,\theta = \left(\nabla^2\theta\right)\ /Re.Pr \tag{4}$$

Where *Re*, *Pr* are Reynolds, and Parndtl numbers respectively.

3.3 Continuity Equation:

The solvent region follows the continuity equation as:

$$\frac{1}{R}\frac{\partial}{\partial R}(RU) + \frac{1}{R}\frac{\partial V}{\partial \Phi} + \frac{\partial W}{\partial Z} = 0 \tag{5}$$

3.4 Mass Transport Equation

The mass transport in the solvent region is governed by:

$$(U.\nabla)C = \ \left(\nabla^2 \mathrm{C}\right)\ /Re.Sc \tag{6}$$

Where Schmidt number (*Sc*) defines the solutal diffusion coefficient.

3.5 Growth Interface Equation

The growth velocity (v_{eff}) which is the interface displacement rate and is a modified version of Helmers, Schilz, Bahr, and Kaysser (1995) and is computed by solving the mass balance equation coupled with the GeSi binary phase diagram.

$$v_{eff} = \frac{v_z}{2}\left[1 - \frac{\nabla \mathrm{c_s}}{\nabla\theta}\left(\frac{\partial T_L}{\partial c}\right)_{\mathrm{c_s/k}}\right]^{-1} \tag{7}$$

Where v_z is the pulling rate, $\nabla \mathrm{c_s}$ is the dimensionless concentration gradient, $\left(\frac{\partial T_L}{\partial c}\right)_{\mathrm{c_s/k}}$ is the slope of the liquidus, $\nabla\theta$ is the dimensionless temperature gradient. For this study, the typical values give $v_{eff} \approx v_z$, by considering the pulling rate v_z in this modeling is set to 0.069 μm/s and is an input parameter in this model.

4 Solution Technique and Mesh Sensitivity Analysis

Finite element method has been utilized in this study and the model is divided into elements and ultimately into nodes to help evaluate and analyze the velocities, temperature, silicon concentration, and pressure by using FIDAP from FLUENT (2004) which is commercial software. Mesh sensitivity analysis was conducted to establish an optimum number of nodes for this study. As can be read from the Tab.1, a 40 x 288 mesh reliably meets the computational requirements for simulation. The reliability of a model depends on the number of elements and nodes it is built on. This model contains over fourteen thousands nodes and Galerkin finite element method of approximation was used for this analysis in the solvent region as defined by FIDAP (1999). The governing equations then were solved simultaneously and criteria for convergence which checks two successive time steps to meet $\frac{||\triangle u_i||}{||u||} \leq \varepsilon_u$ where u_i represents the pressure, temperature, velocities and silicon concentration, along r, ϕ and z directions for each node were considered.

Table 1: Mesh Sensitivity analysis

Item	**Mesh Density(Grids)** (Circumferential x Axial)	**Average Heat Flux** (Dimensionless Values) From FIDAP
1	10 x 288	20.8806
2	20 x 288	20.7635
3	30 x 288	20.6014
4	40 x 288	20.4918
5	50 x 288	20.4909
6	60 x 288	20.4940
7	70 x 288	20.4978
8	80 x 288	20.4956

5 Results and Discussion

An axial thermal gradient of 60K/cm has been shown and observed by other researchers such as; Paul (1999), Coriell and Sekerka (1997), Barat, Duffar, and Garandet (1998) in their experiments and studies. In this study we discuss different axial temperature gradient from 60K/cm to 30K/cm by applying a linear temperature profile on the model. Fig. 2 and Fig. 3 represent the silicon composition distribution and flow velocities respectively along the vertical axis of the model passing through the centre of the solvent region for a) 60K/cm, b) 50K/cm, and c) 40K/cm respectively. The excess heat in the first 3 set up as shown in Fig. 3 has caused the strong convection mostly in the upper zone of the sample. Fig. 4

shows silicon distributions where a) 35K/cm, b) 32K/cm, and c) 30K/cm temperature gradients were applied respectively on the solvent region. It is clear that in the case of 35K/cm, the silicon composition is in 25 at% for nearly 20mm of the model which is the targeted value. At the same time by observing both Fig. 3 and Fig. 5, one can see that the flow velocity is considerably low especially in the case of applied 35K/cm and more noticeably for the first 20mm above the growth interface of the model. With this flow velocity (27 μm/s), the thermal Peclet number $(Pc)_T = Re\ .Pr \approx 0.01$ which is much less than 1, and solutal Peclet number $(Pc)_S = Re\ .Sc \approx 143$ this is a good indicator and shows that the mass diffusion is dominating in the solvent region in general and the first 25mm above the growth interface specifically.

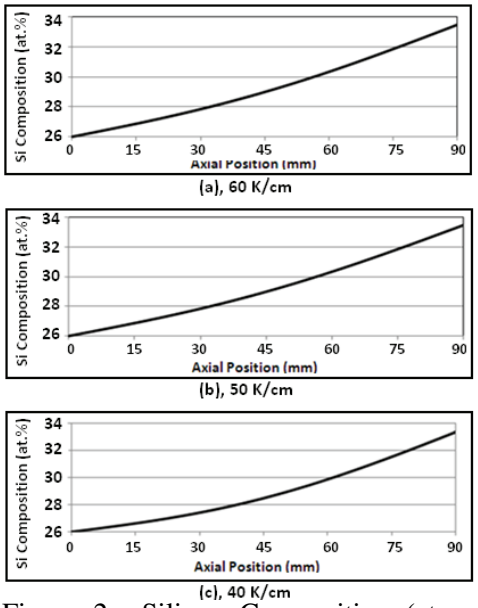

Figure 2: Silicon Composition (at. %) along the Vertical Axis a) Applied 60K/cm axial temperature gradient b) Applied 50K/cm axial temperature gradient c) Applied 40K/cm axial temperature gradient

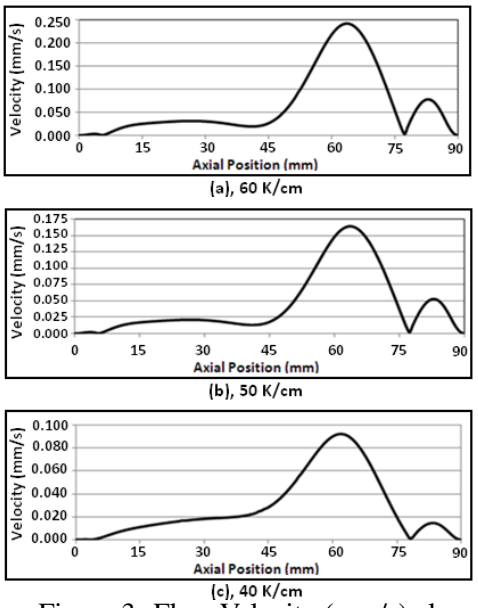

Figure 3: Flow Velocity (mm/s) along the Vertical Axis a) Applied 60K/cm axial temperature gradient b) Applied 50K/cm axial temperature gradient c) Applied 40K/cm axial temperature gradient

The model (solvent region only) is then sliced and investigated at one millimeter intervals in order to observe the temperature distribution in the radial direction more closely.

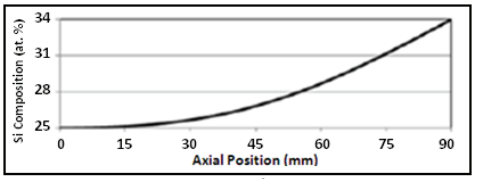

(a), 35 K/cm

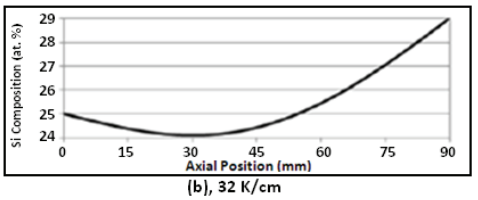

(b), 32 K/cm

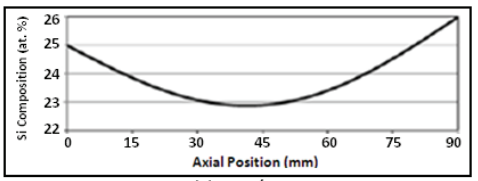

(c), 30 K/cm

Figure 4: Silicon Composition (at. %) along the Vertical Axis a) Applied 35K/cm axial temperature gradient b) Applied 32K/cm axial temperature gradient c) Applied 30K/cm axial temperature gradient

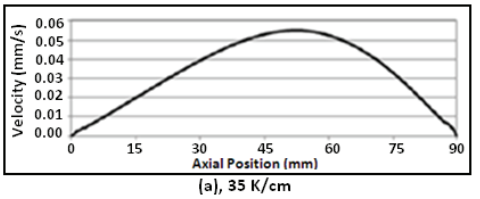

(a), 35 K/cm

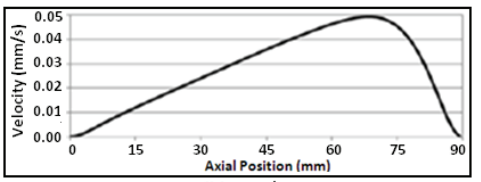

(b), 32 K/cm

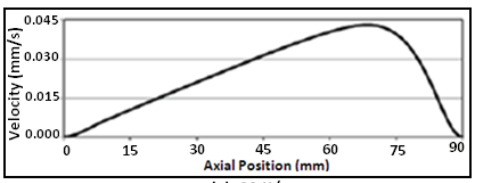

(c), 30 K/cm

Figure 5: Flow Velocity (mm/s) along the Vertical Axis a) Applied 35K/cm axial temperature gradient b) Applied 32K/cm axial temperature gradient c) Applied 30K/cm axial temperature gradient

It was seen that by slicing the solvent region into 1mm intervals in the axial direction, the temperature distribution in this region follows two regimes, Fig. A1 in Appendix "A". The lower zone which is from the growth interface up to 40 mm above it and upper zone from 40 mm to dissolution interface at 90 mm of the model. As it is shown in the Tab. 2, the maximum radial temperature difference happens at 40 mm above the growth interface which indicates a 0.06 K/cm gradient. These radial temperature differences can be formulized by applying bilinear interpolation as follow:

For Lower Zone:

$$\triangle T\,(r,z) = 0.04685\ z\ (1-2r) \tag{8}$$

and for Upper Zone:

$$\triangle T\,(r,z) = 0.135 - 0.27r - 0.035z + 0.075rz \tag{9}$$

Table 2: Radial Temperature Differences along Vertical Axis of the Model Covering Lower and Upper Zones

Item	Distance from growth interface (mm)	Radial temperature difference (ΔT)
1	0	0
2	1	0.0023
3	2	0.0042
4	3	0.0065
5	4	0.0085
6	5	0.0097
7	10	0.0250
8	20	0.0500
9	30	0.0700
10	40	0.0750
11	50	0.0600
12	60	0.0350
13	70	0.0060
14	80	0.0025
15	85	0.0014
16	89	0.0010
17	90	0.0000

6 Conclusion

Given the chemical composition of the solvent region, the pulling rate, and thermal gradient axially and radially are also playing a strong role in the process of crystal growth Duhanian, Duffar, Marin, Dieguez, Garandet, and Dantan (2005). As discussed, with the proposed axial temperature gradient and pulling rate, a uniform silicon distribution and a diffusion dominant (Pe_T le 1) segment of the model can be obtained and a homogeneous single bulk crystal can be produced. This finding can be considered as an alternative to other means for suppressing the convective motion in the crystal growth process. Although the process is relatively slow as a result of the proposed pulling rate but from the economical point of view, it is much more affordable compare to microgravity setting, and or application of magnetic field whether it is rotating or static.

Acknowledgement: The Authors appreciate the support of Mechanical and Industrial Engineering Departments of both ALHOSN and Ryerson universities.

Appendix A

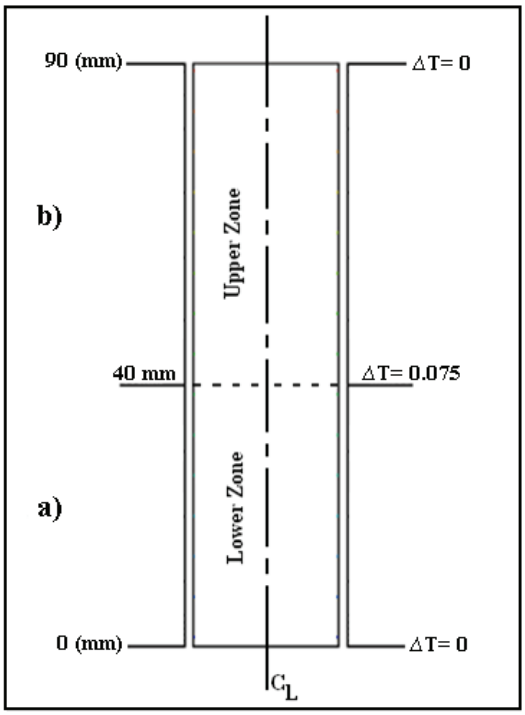

Figure A-1: Two zones of radial temperature gradient variations in solvent region (35K/cm axial thermal gradient case)

References

Barat, C.; Garandet, J. P. ; Duffar, T. (1998): Estimation of the curvature of the soild-liquid interface during Bridgman crystal growth. *Journal of Crystal Growth,* vol. 194, pp. 149-155.

Chang, C. J.; Brown, R. A. (1983): Radial segregation induced by natural convection and melt/solid interface shape in vertical Bridgman growth. *Journal of Crystal Growth*, vol. 63, pp. 343-364.

Chong, E. C.; Wilcox, W. R. (1974): Control of interface shape in the vertical Bridgmen-Stockbarger technique. *Journal of Crystal Growth*, vol. 21, pp. 135-140, North Holland Publishing Co.

Cor iell, S. R.; Sekerka, R. F. (1979): Lateral solute segregation during unidirectional solidification of a binary alloy with a curved solid-liquid interface. *Journal of Crystal Growth*, vol. 46, pp. 479-482.

Duhanian, N.; Duffar, T.; Marin, C.; Dieguez, E.; Garandet, J. P.; Dantan, P.; Guiffant, G. (2005): Experimental study of the solid-liquid interface dynamics and chemical segregation in concentrated semiconductor alloy Bridgman growth,*Journal of Crystal Growth*, vol. 275 (3- 4), pp. 422- 432.

Feonychev, A. I. (2004): Effect of A Rotating magnetic Field on Convection Stability and Crystal Growth in Zero Gravity and on the Ground. *Journal of Engineering Physics and Thermodynamics.* Vol. 77, No.4, pp. 731-742.

FIDAP, (1999): user manual.

FLUENT, (2004): user manual.

Fu, T. W.; Wilcox, W. R. (1980): Influence of insulation on stability of interface shape and position in the vertical Bridgman-Stockbarger technique. *Journal of Crystal Growth*, vol. 48, pp. 416.

Helmers, L.; Schilz, J.; Bahr, G.; Kaysser, W. A. (1995): Macrosegregation during Bridgman growth of $Ge_{1-x}Si_x$ Mixed crystals. *Journal of Crystal Growth*, vol. 154(1-2), pp. 60 - 67.

Jasinsky, T.; Witt, A. F. (1984): Heat transfer analysis of the Bridgman-Stockbarger configuration for crystal growth:II. Analytical treatment of radial temperature variations. *Journal of Crystal Growth*, vol. 67(2), pp. 173-184.

Meyer, S; Ostrogorsky, A. G. (1997): Forced convection in vertical Bridgman configuration with the submerged heater. *Journal of Crystal Growth*, vol. 171 (3-4), pp. 566-576.

Nikitin, S. A.; Polezhayev, V. I.; Fedyushkin, A. I. (1981): Mathematical simulation of impurity distribution in crystals prepared under microgravity conditions. *Journal of Crystal Growth*, vol. 52, pp. 471-477.

O'Mara, ; William, C. (1990): *Handbook of Semiconductor Silicon Technology*, William Andrew Inc., ISBN 0815512376, pp. 349-352.

Paul, D. J. (1999): *Advanced materials,* vol. 11(3), pp. 191-204.

Walker, J. S. (1998): *Journal of Crystal Growth*, 192, pp. 318-327.